

EL NIÑO MODOKI IMPACTS ON AUSTRALIAN RAINFALL

Andréa S. Taschetto*, Alexander Sen Gupta, Caroline C. Ummenhofer and Matthew H. England
Climate Change Research Centre (CCRC), University of New South Wales, Sydney, Australia

1. INTRODUCTION

Events related to the recently-termed El Niño Modoki have become more frequent than traditional El Niños over the past few decades (Ashok et al., 2007). A Modoki event is characterized by warm sea surface temperature (SST) anomalies in the central Pacific straddled by colder anomalies to either side. Although the mechanisms behind El Niño Modoki episodes are still elusive, it is clear that their impacts on regional climate are distinct from those related to a canonical El Niño (Weng et al., 2007).

Wang and Hendon (2007) showed that the strongest recorded El Niño event of 1997/1998 was associated with near-normal rainfall over Australia, while the modest event of 2002/2003 resulted in near-record drought across the continent. Interestingly, the 2002/2003 El Niño event exhibited its warmest SST anomalies in the central equatorial Pacific, characteristic of a Modoki, instead of in the east, as in the 1997/1998 El Niño. This suggests that Australian rainfall may be more sensitive to positive SST anomalies near the date line rather than corresponding anomalies in the eastern Pacific.

In this study we (1) investigate the effect of El Niño Modoki events on Australian rainfall during austral summer and autumn, using observations; (2) assess the sensitivity of Australian rainfall via perturbation experiments with idealized SST configurations in an atmospheric general circulation model; and, (3) examine whether the IPCC climate models can represent El Niño Modoki events.

2. DATA AND METHODS

The following datasets are used in this study: (1) the global SST analysis from the Hadley Centre (HadISST1, Rayner et al., 2003); (2) rainfall from the Australian Bureau of Meteorology (BoM); (3) winds, specific humidity and vertical velocity from the National Center for Environmental Prediction / National Center for Atmospheric Research (NCEP/NCAR) Reanalysis. We confine our analysis to the more reliable era, the period from 1979 to 2005. The moisture flux and its divergence were calculated for both observations and simulations. We used Singular Value Decomposition (SVD) and composite analyses to show the relationship between observed rainfall and the Modoki SST pattern.

The NCAR Community Atmospheric Model (CAM3) is used to assess the sensitivity of Australian rainfall to different locations of SST warming in the Pacific. The AGCM was forced with climatological monthly SST values. In addition, an idealized 1°C positive SST

anomaly was added along the equatorial Pacific, bounded between 10°N and 10°S and longitudinally located in: (1) the eastern Pacific, from 120°W to 80°W; (2) the central-eastern Pacific, from 160°W to 120°W; (3) the central-western Pacific, from 160°E to 160°W; and, (4) the western Pacific, from 120°E to 160°E. We analyze the rainfall and moisture flux responses over the Australian region.

The IPCC climate models were obtained from the Program for Climate Model Diagnoses Intercomparison (PCMDI). We analyze the last 20 years of the 20th century control run through regression analyses and Empirical Orthogonal Function (EOF) rotated by the Varimax method.

3. RESULTS

3.1 A preliminary assessment

The Modoki SST pattern appears as the second mode of interannual variability in an EOF analysis over the tropical Pacific, accounting for approximately 12% of the total variance (Ashok et al., 2007). Taschetto and England (2009) have shown that when an SVD analysis is performed with seasonal Pacific SST and Australian rainfall data, the Modoki pattern actually appears as the leading mode of variability. It is associated with dry conditions across the continent during austral autumn (MAM).

The coupled pattern remains very similar when the SVD is computed with the seasonal December to February (DJF) SST and MAM rainfall. As a result of this we will focus our analysis on the austral summer (DJF) and autumn (MAM) seasons, when Modoki strongly affects Australian climate.

3.1 Observations

Figure 1 shows a composite analysis for the El Niño Modoki events of 1979/1980, 1986/1987, 1990/1991, 1992/1993, 1994/1995 and 2002/2003. The selection of these events is in agreement with Ashok et al. (2007). For comparison, Figure 1 also shows the composited fields for the classical El Niño events of 1982, 1987 and 1997, but during SON when ENSO impacts are stronger in Australia. A marked difference in the rainfall distribution is seen over Australia: while classic El Niños are associated with a significant reduction in rainfall over northeastern and southeastern Australia during September to November (SON), the Modoki events appear to drive a large-scale decrease in rainfall over northwestern and northern Australia during MAM.

* Corresponding author address: Andréa S. Taschetto, Climate Change Research Centre (CCRC), University of New South Wales, Sydney, NSW, 2052, Australia.
e-mail: a.taschetto@unsw.edu.au

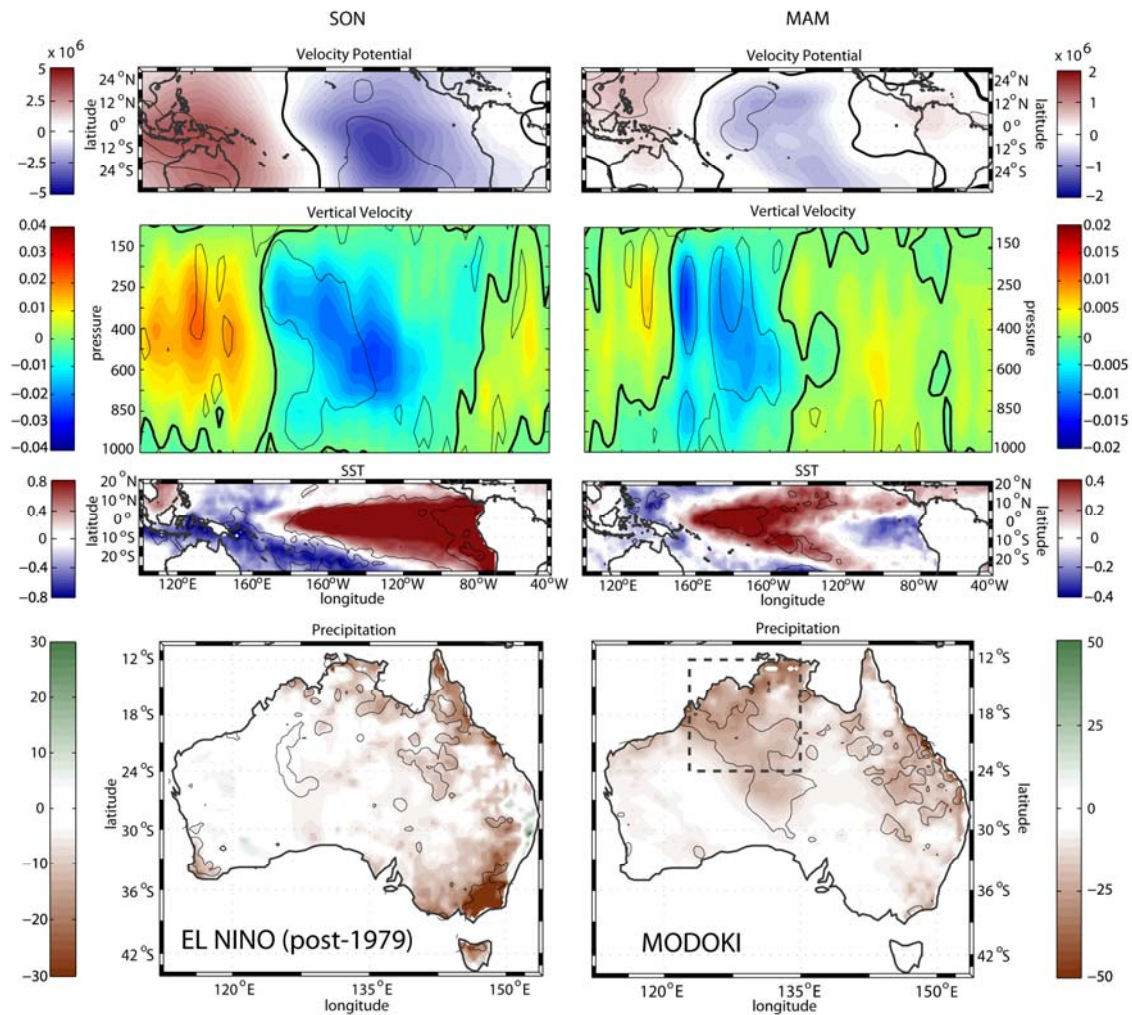


Figure 1. Composites of velocity potential at 200hPa (m^2/s), vertical velocity (Pa/s) averaged over $10^{\circ}N-10^{\circ}S$, SST ($^{\circ}C$) and precipitation (mm/month) during SON for ENSO: 1982, 1987 and 1997 (left panel) and during MAM for the El Niño Modoki: 1980, 1987, 1991, 1995, 2003 (right panel). The area within the black dashed box in the lower right panel is averaged to create the rainfalltime-series used in Figure 3. From Taschetto and England (2009).

For the Modoki composites, the vertical velocity shows upward motion through the deep troposphere centered at $180^{\circ}W$, west of the rising air in the conventional ENSO-composite circulation. The velocity potential at 200hPa also confirms that anomalous divergence is shifted to the west associated with ascending air over the warm central Pacific SST anomalies. The anomalous divergence in the central-west Pacific causes convergence and thus subsidence over South America and the Indonesian region, forming the double Walker Cell described by Ashok et al. (2007).

Interestingly, when the SVD and composite analyses are carried out for the averaged summer season, northern Australia does not show strong dry conditions (not shown). This raises the question of why DJF rainfall does not show negative anomalies as in MAM for the same Modoki signature. To answer

this we examine the monthly evolution of Australian rainfall.

Figure 2 depicts the December to March rainfall anomalies composited for El Niño Modoki events. It reveals the opposite signal in January and February compared to December and March. The composited rainfall anomalies were also compared with those from the CPC Merged Analysis of Precipitation (CMAP), the NCEP/NCAR and the ECMWF (ERA40) Reanalyses (Fig. not shown), and they are in close agreement with the precipitation pattern derived from BoM.

Therefore, the SVD and composite analyses for the averaged summer season did not appear in the previous analysis because the negative and positive anomalies offset each other, giving a false impression that Modoki does not have a strong impact on Australian climate during this season.

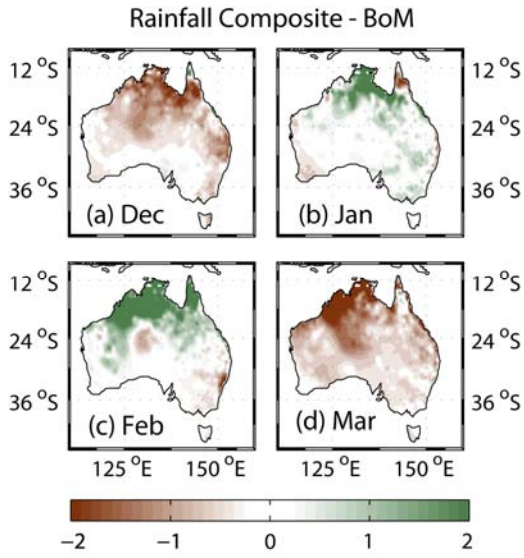


Figure 2. Rainfall anomaly composite for Modoki years from December to March (1979/1980, 1986/1987, 1990/1991, 1992/1993, 1994/1995 and 2002/2003). Adapted from Taschetto et al. (2009).

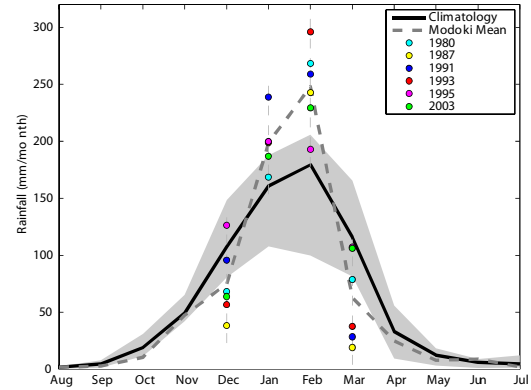


Figure 3. Annual cycle of rainfall in northwestern Australia. Black thick line represents the climatology and the dashed line indicates the anomalous behavior during El Niño Modoki years. Individual December to March months for Modoki events are highlighted with circles. Values outside the gray shades area are significant at the 95% level based on a Monte Carlo test. Adapted from Taschetto et al. (2009).

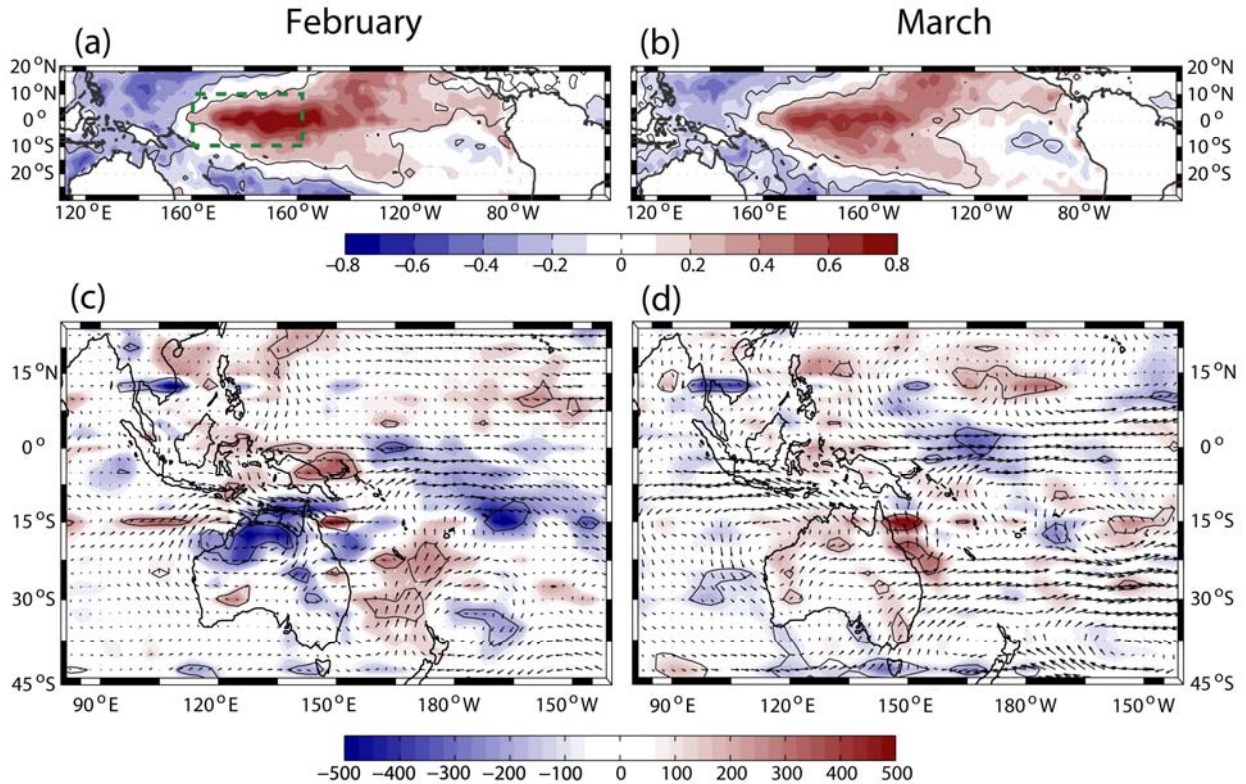


Figure 4. Composites of SST (a-b), moisture flux and divergent moisture flux anomalies for observations (c-d) during Modoki events in February (left panels) and March (right panels). Areas within the thin black contours are significant at the 95% level. The dashed box in (a) represents the area where the SST anomaly was used to force the central-west Pacific experiment. Units are in degrees Celsius, $\text{kgm}^{-1} \text{s}^{-1}$ and kg s^{-1} , respectively. Adapted from Taschetto et al. (2009).

The reduced rainfall in December and March and increase in January and February is a robust signal across almost all Modoki events. This can be seen in Figure 3 that shows the annual rainfall cycle over northern Australia (12°S - 24°S , 120°E - 135°E) for the Modoki years compared to the climatology.

The Modoki-related anomalies thus lead to a shortening of the monsoon season over northern Australia, with an associated intensification of precipitation in January and February. In other words, Modoki events can be associated with a late monsoon onset and an early monsoon termination over Australia. These findings have been documented by Taschetto et al. (2009).

Table 1. Simulated rainfall in northern Australia in response to an SST anomaly of 1°C imposed in the east, central-east, central-west and west Pacific Ocean. Values are shown as anomalies about the mean in the control experimental ensemble set.

| SST warming | February (mm) | March (mm) | Difference (Feb-Mar) |
|--------------|---------------|--------------|----------------------|
| East | 25.2 | -6.7 | 31.9 |
| Central-East | 16.3 | -0.4 | 16.7 |
| Central_West | 28.8 | -11.5 | 50.3 |
| West | 27.3 | 5.6 | 21.7 |

To investigate the mechanisms behind the increased precipitation, we calculated the vertically integrated moisture flux from the surface to 500hPa and its associated divergence field. Figure 4 reveals that intensified rainfall in February results from a strong convergence of moisture caused by an anomalous anticyclonic circulation over northwestern Australia. On the other hand, Australia experiences a divergence of moisture in March, which leads to less precipitation. The rainfall decrease in March is exacerbated by the subsidence of the western branch of the anomalous Walker circulation during Modoki events. However, anomalous subsidence is not evident over northern Australia in February (Figure not shown).

3.2 NCAR Atmospheric Model

The sensitivity of Australian rainfall anomalies to the different locations of warming along the equatorial Pacific is examined by applying warm anomalies at different tropical locations in numerical experiments. The idealized experiments show an overall rainfall increase in February and a decrease in March. The strongest rainfall response in February (wet) and March (dry) is seen when the positive SST anomaly forcing is located in the central-west Pacific (Table 1). This corroborates Wang and Hendon (2007)'s finding that Australian climate is sensitive to the location of SST anomalies in the tropical Pacific. In addition, SST warming around the Dateline, typical of Modoki events, tends to impact more strongly on Australian rainfall than the positive anomalies located in the eastern Pacific, as found during traditional El Niño events. Figure 5a shows the change in the rainfall frequency distributions in the central west perturbed experiment relative to the control.

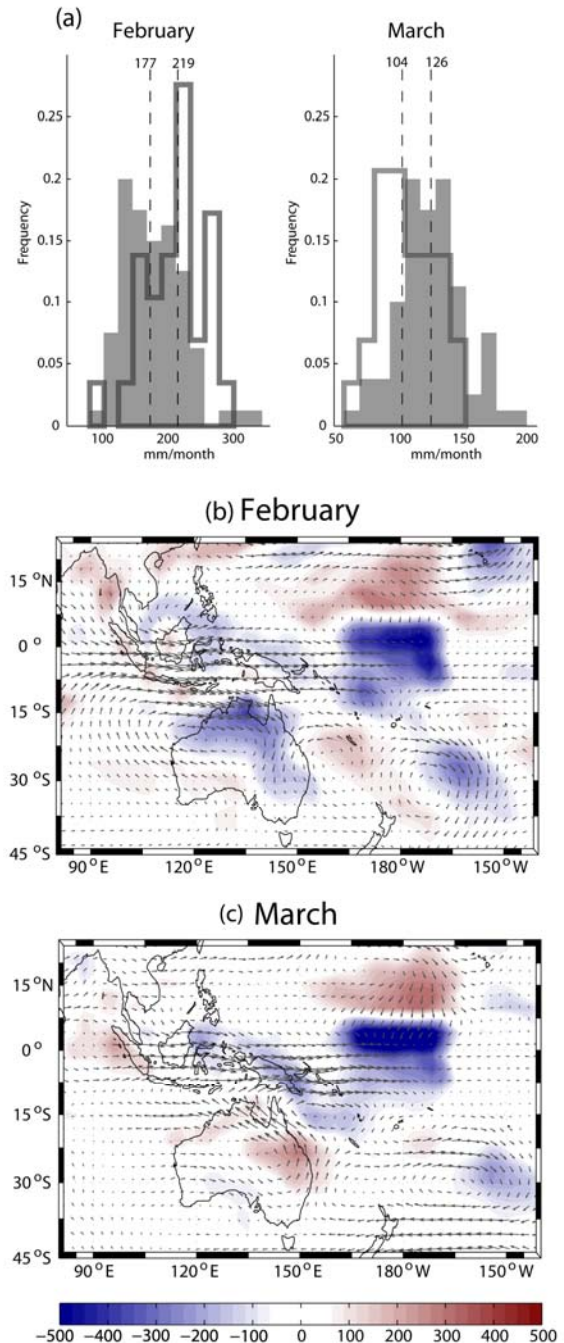


Figure 5. (a) Histograms of rainfall for the central-west Pacific warming experiment (dark contour) and the control (gray shaded) in February (left) and March (right). The dashed lines represent the median rainfall. The median (number above dashed line) of the warming experiment are statistically different at the 0.05 level from those of the control, based on both a Student t-test and a Wilcoxon-Rank Sum test for normal and non-parametric distributions, respectively. Simulated moisture flux ($\text{kgm}^{-1} \text{s}^{-1}$) and divergent moisture flux (kg s^{-1}) anomalies for the central-west Pacific warming experiment, (b) February and (c) March. Adapted from Taschetto et al. (2009).

The experiment forced with the SST warming in the central-west Pacific captured well the convergence of moisture flux in February (Figure 5c) and the divergence over Australia in March (Figure 5d). This result suggests that a warming solely in the central-western Pacific may be sufficient to drive the monsoonal changes observed in Modoki years.

3.3 IPCC Climate Coupled Models

Nineteen coupled models were examined from the PCMDI data base, i.e. BCCR BCM2.0, CCCM3 T47, CCCM3 T63, CNRM CM3, CSIRO Mk3.0, CSIRO Mk3.5, GISS-EH, IAP FGOALS, INGV ECHAM4, INM CM3.0, IPSL CM4, MIROC Hires, MIROC Medres, MIUB ECHO-G, MRI CGCM2.3, NCAR CCSM3, NCAR PCM1, UKMet HadCM3, UKMet HadGem1.

For most of these models, the traditional El Niño appears as the leading EOF mode of variability in the tropical Pacific SST anomalies. However, a simple EOF analysis reveals that NONE of these models simulate an El Niño Modoki pattern in the tropical Pacific.

A rotated EOF analysis (Figure not shown) shows that two models have a somewhat Modoki-like pattern as the second mode of variability: MIROC Medres and IPSL CM4. ENSO remains the leading mode in these models. The fact that the Modoki-like pattern appears as the second mode in a rotated EOF analysis lends some weight to the idea that this phenomenon is actually part of the ENSO evolution. Their associated PC time series are significantly correlated with the NINO3 and Modoki Indices calculated in these models (Table 2). Although a Modoki-like pattern is captured as the second mode in the rotated-EOF analysis, the corresponding simulated rainfall signature over Australia does not however resemble a shorter and intensified monsoon regime.

Table 2: Correlation coefficients between the time series of the leading two EOF Principal Components (PC) and Nino 3 and Modoki Indices.

| Model | PC1 x NINO3 | PC2 x Modoki |
|--------------|-------------|--------------|
| MIROC Medres | 0.89 | 0.68 |
| IPSL CM4 | 0.97 | 0.57 |

4. CONCLUSIONS

Changes in the magnitude and location of El Niño-induced-SST warming have significant implications for Australian rainfall. In this study we show that Modoki impacts Australian rainfall differently to ENSO. It is associated with below-normal rainfall over northern Australia in December and March to May and intensified precipitation during January and February. This leads to a shorter and strengthened monsoon season.

The increase in precipitation in January and February is caused by anomalous convergence of moisture flux onto the continent. On the other hand, the decreased rainfall in the other months occurs by divergence of moisture and the subsidence by the western branch of the altered Walker circulation during Modoki events. The reason why the subsidence is not seen in February is still unclear.

Using numerical experiments with the NCAR CAM3 model, we show that Australian rainfall responds more strongly to a warming located in the equatorial Pacific around the date line than the warming in the east, as typical of traditional El Niños. The experiment with warming in the central-west Pacific simulated a convergence of moisture flux in February and the moisture divergence in March, suggesting that the Modoki – related SST warming is one of the factors modulating the Australian monsoon variability.

Finally we show here that an obvious Modoki signature is not evident in the IPCC climate models.

5. REFERENCES

- Ashok, K., S. K. Behera, S. A. Rao, H. Weng, and T. Yamagata, 2007: El Niño Modoki and its possible teleconnection. *J. Geophys. Res.*, 112 (C11007), doi:10.1029/2006JC003798.
- Taschetto, A. S. and M. H. England, 2008: An analysis of late 20th Century trends in Australian rainfall. *Int. J. Climatol.*, doi:10.1002/joc.1736.
- Taschetto, A. S. and M. H. England, 2009: El Niño Modoki impacts on Australian rainfall. *J. Clim.*, in press.
- Taschetto, A. S., C. C. Ummenhofer, A. Sen Gupta and M. H. England, 2009: The effect of anomalous warming in the central Pacific on the Australian monsoon. *Geophys. Res. Lett.*, submitted.
- Wang, G. and H. H. Hendon, 2007: Sensitivity of Australian rainfall to inter-El Niño variations. *J. Clim.*, 20, 4211–4226.
- Weng, H., K. Ashok, S. K. Behera, S. A. Rao, and T. Yamagata, 2007: Impacts of recent El Niño Modoki on dry/wet conditions in the Pacific rim during boreal summer. *Clim. Dyn.*, 29, 113–129.